Micro-structural and tensile strength analyses on the magnesium matrix composites reinforced with coated carbon fiber

Z. L. Pei · K. Li · J. Gong · N. L. Shi ·
E. Elangovan · C. Sun

Abstract Magnesium matrix composites reinforced with SiO_2 coated carbon fibers have been investigated, with an emphasis given on the relation between the material strength and interfacial microstructure. The composites were studied as a function of aluminium (Al) content that is varied between 0 and 9 wt%. The obtained results indicate that the reactivity at the C/Mg–Al interface of the composite can be controlled by varying the Al content. The low Al content in C/Mg–1Al has been completely dissolved in the matrix with no segregation even after solidification, leading to the best mechanical performance. If the Al content is increased to ≥3 wt% (composites such as C/AZ31 and C/AZ91), the SiO_2 coatings are fully depleted due to an extensive formation of carbides at the interface. The precipitates are further identified as Al_2MgC_2 phase that is similar to binary carbide Al_4C_3. SiO_2 coating on the fiber layer prior to fabrication of composite is found to be a promising way to suppress the carbide formation and enable the use of Mg–Al matrix with appropriate Al content.

Introduction

The emerging structural materials of carbon fiber reinforced metal matrix composites (MMCs) exhibit high specific strength and stiffness, good thermal conductivity, and a near-zero thermal expansion coefficient. However, their commercial utilization is still restricted when compared to polymer composites or conventional structural materials (such as steel, etc.), since they suffer from several material inherent deficiencies like wetting, interfacial chemical reaction, cost, and galvanic corrosion [1, 2].

It is well established that the interfacial issues are key points in C/Mg system to obtain the high-performance composites. On the contrary to C/Al composite, the C/Mg system is non-reactive with a weak interface bonding between fibers and matrix. Hitherto, two kinds of remedies were presented to increase the interfacial adhesion, namely adding of carbide-forming element of Al or modifying the fiber surface [3, 4]. With respect to modification of the fiber surface, the used coatings can minimize reaction layers in the interfaces in addition to the increase in wettability. Moreover, the use of coatings can also decrease the desired filtration pressure to avoid the fiber disarrangement or damage. However, the existing cast technology can overcome the poor wettability by using higher pressure (several 100 MPa). Additionally, C/Mg–Al composites with different Al contents in the matrix show diverse interfacial characteristics and material strength. The majority of literature concerning C/Mg composites deals with the increasing wettability through the deposition of coatings such as silicon dioxide—SiO_2 [3, 5], titanium nitride—TiN [4] or silicon carbide—SiC [6] over fiber surface prior to composite fabrication. However, there are some conflicts with the obtained results regarding the usage of interlayer [7, 8]. Therefore, a detailed investigation is demanded to explore and achieve an effective control over the interface.

In this study, a thin SiO_2 layer is chosen as coating material whereas commercially available pure magnesium and its Al alloys are applied as the matrices. The fracture behavior and mechanical property of C/Mg–Al composites are discussed

Z. L. Pei · K. Li · J. Gong (✉) · N. L. Shi · C. Sun
Institute of Metal Research, Chinese Academy of Sciences,
Shenyang 110016, China
e-mail: jgong@imr.ac.cn

Z. L. Pei
e-mail: zlpei@imr.ac.cn

E. Elangovan
CENIMAT/I3N, Materials Science Department, FCT-UNL,
2829-516 Caparica, Portugal

with particular attention to the interfacial characteristics. Furthermore, the obtained results are well interpreted with the existing findings. The primary aim of this study is to explore the interfacial problems in C/Mg composites and the obtained results may contribute to the related research on this topic.

Experimental

The C/Mg composites were fabricated by a gas pressure infiltration technology using different matrices of commercially pure (c.p.) Mg, Mg–Al, AZ31, and AZ91 with Al content of approximately 0, 1, 3, and 9 wt%, respectively. The reinforcement used in this experiment is T-300B carbon fiber with a tensile strength of 3530 MPa. To improve the poor wettability of C/Mg system, the fibers were pre-coated with a thin SiO_2 layer ($\sim$30 nm thick) prior to infiltration. Sol–gel method is used to coat SiO_2 layer and the details of which are described elsewhere [9, 10]. Carbon fibers were also extracted from cast composites by dissolving the matrix with 30 vol.% HNO_3 aqueous solutions, in order to investigate the variation in the material strength and surface microstructures. The tensile strength of carbon fibers was estimated through a standard mechanical machine according to the testing standard (ASTM D4018-1999). The number of testing was 50 with a gauge length of 25 mm, and the results were evaluated by the Weibull distribution theory.

All the composites were prepared with a fiber volume percent of approximately 35% and examined in the as-received state. Longitudinal tensile strength was conducted at a constant cross-head speed of 0.5 mm/min by a Zwick testing machine. A JEOL JSM6301F scanning electron microscope (SEM), operating at 3 kV, was used to observe the fractures on the surface. Transmission electron microscopy (TEM) analysis was carried out using a Philips CM20 transmission electron microscope operating at 200 kV. Elemental analysis was performed through energy dispersive spectroscopy (EDS), an attachment that is available with the TEM apparatus. Specimens were prepared in the usual way by cutting thin slice of 3 mm in diameter and then reducing the thickness to about 40 μm by planar grinding and dimpling, which was followed by ion milling (Ar^+, 5 kV) down to electron transparency.

Results and discussion

Strength analysis for the coated C/Mg–Al composites

In principle, the SiO_2 coating would not only prevent the degradation of fibers following the low temperature processing, but also avoid fiber sticking to achieve the homogeneous coating. As shown in Fig. 1, the SiO_2 coated carbon fibers are completely infiltrated by the different
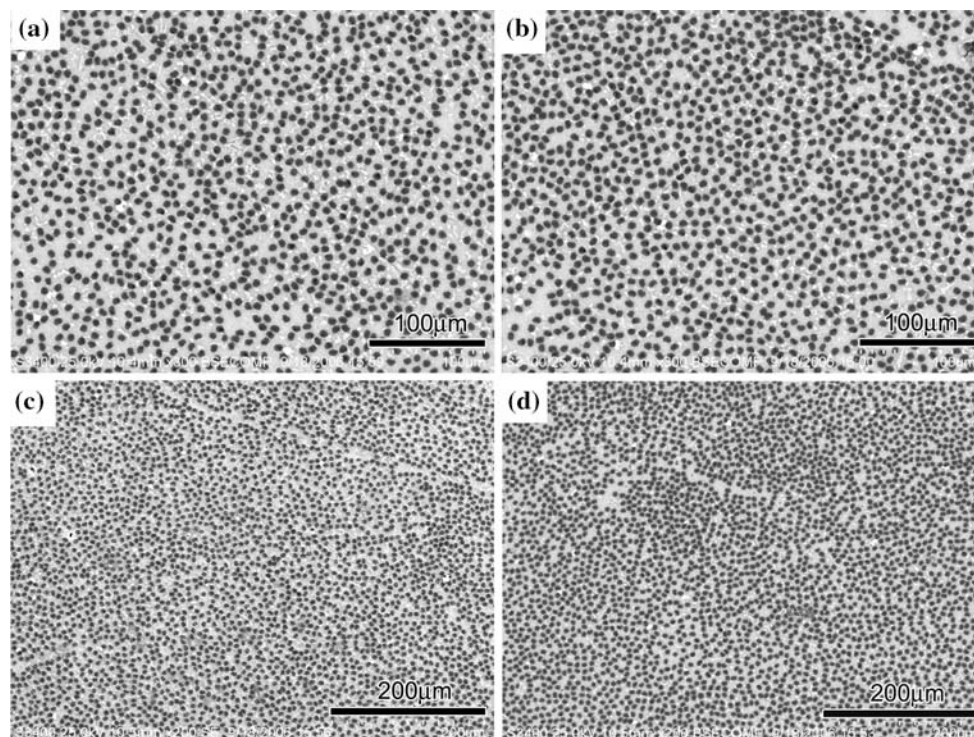

Fig. 1 SEM micrographs showing the transverse distributions of carbon fibers in **a** C/c.p. Mg; **b** C/Mg–1Al; **c** C/AZ31, and **d** C/AZ91 composites, respectively
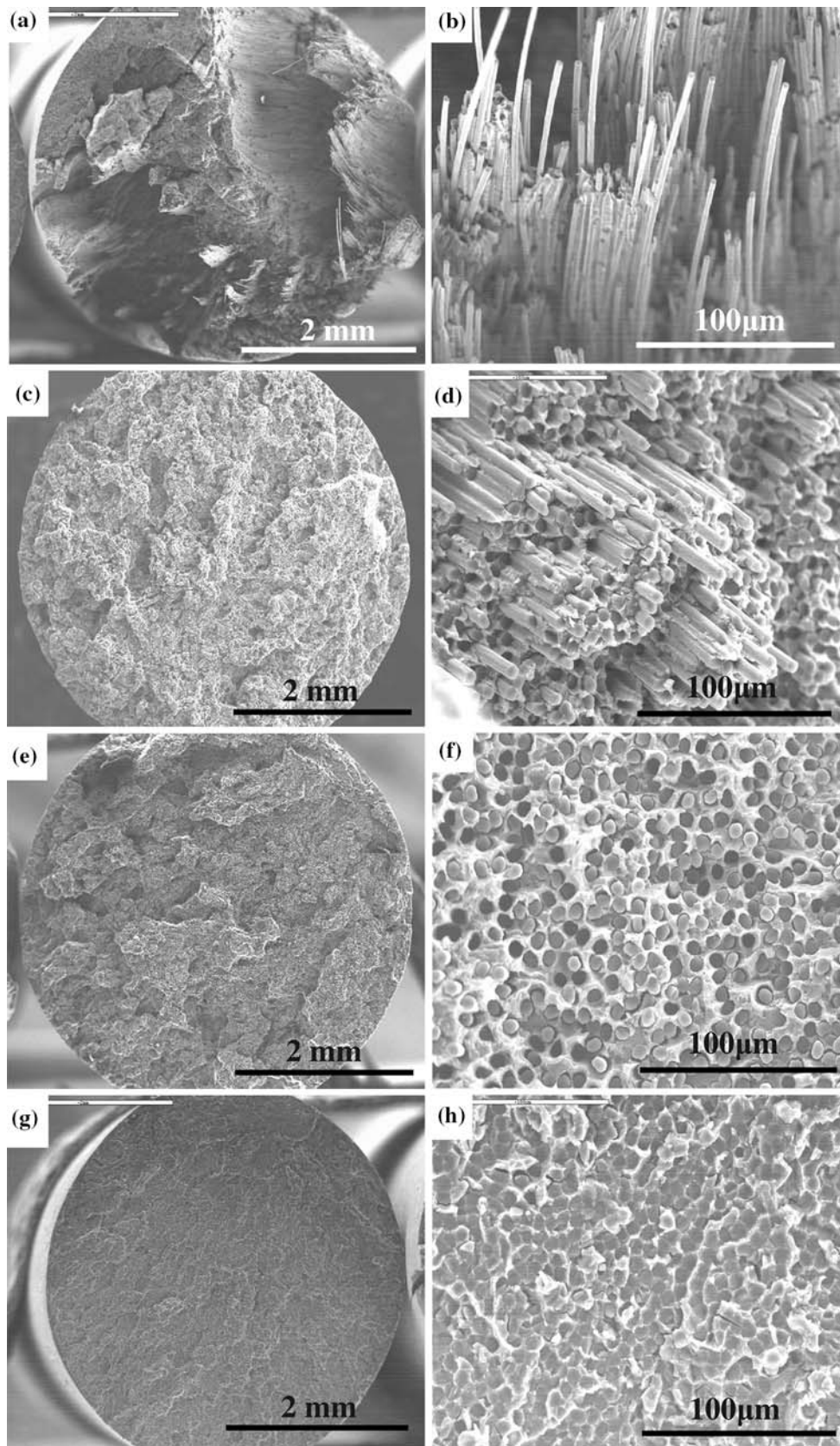
Fig. 2 SEM images of fracture surfaces—Left column of the figure shows the full cross-sectional view of the sample and the right column shows the magnified view: **a** and **b** for C/c.p. Mg, **c** and **d** for C/Mg–1Al, **e** and **f** for C/AZ31, **g** and **h** for C/AZ91

matrices and are uniformly distributed in all the composites, with no fiber contact, voids or macro-cracks.

The microstructures obtained from cross-sectional view of SEM analysis are shown in Fig. 2. The left column of the figure shows full cross-sectional view whereas those on the right column are the magnified view. For a comparison, the tensile characteristics of C/Mg–Al composites are also presented in Fig. 3. Additionally, the average tensile strength and its respective standard deviation obtained from all the systems are quantified in Table 1. As shown in Fig. 2a, b for the non-reactive C/c.p. Mg system, a considerable fiber pullout is observed and fracture occurs in the form of single fiber, indicating the weak interface bonding as suggested by TEM observation (discussed later). In case of composites with moderate interfacial reactivity (Fig. 2c, d), the observed fracture behavior is in the form of fiber bundle. Furthermore, the C/Mg–1Al composite offers an ultimate tensile strength (UTS) of 612 MPa, which is approximately eight times higher than that of pure Mg matrix produced at the same condition
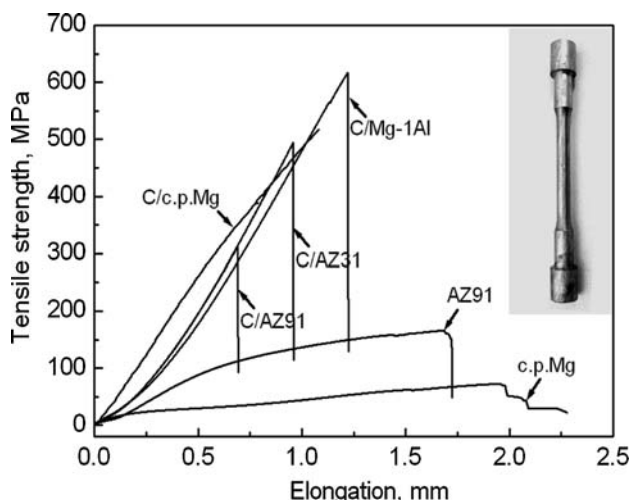

Fig. 3 Tensile behavior of the C/Mg–Al composites compared with the pure Mg matrix produced at the same condition. Insert: the tested cylindrical samples with a gauge length of 25 mm and a diameter of 4 mm

Table 1 Average tensile strength and standard deviation for all the material systems employed

Material systems	Average tensile strength (MPa)	Standard deviation (MPa)
c.p. Mg	72	1.80
AZ91	152	1.72
C/c.p. Mg	501	1.12
C/Mg–1Al	604	1.22
C/AZ31	492	0.96
C/AZ91	310	0.69

(Fig. 3 and Table 1). On the other hand, the highly reactive C/AZ31 and C/AZ91 composites (Fig. 2e–h) show a brittle fracture behavior without any fiber pullout and the obtained material strength is relatively low (Fig. 3 and Table 1). Meanwhile, the ductility of the materials is significantly decreased with the increase in Al content (≥ 3 wt%) in the alloys. Conclusively, performances of the materials are strongly dependent on the interface reactivity that can be controlled by varying the Al content in the matrix. Previous reports [4, 11] on the effect of Al alloying elements on the properties of these composites suggested that the interfacial bonding in C/AM20 (2 wt% Al) composites is moderate and could provide the highest tensile strength. Our preliminary results indicate that the C/Mg–1Al is preferred since it presents proper interface bonding and the best properties over other systems. Therefore, the optimum Al content in the matrix can be further optimized that demands a more detailed investigation.

As the principal reinforced element, the variation in the tensile strength of carbon fibers in MMCs needs to be emphasized. Figure 4 shows the variation in the tensile strength of raw fibers, coated fibers, and the fibers in C/c.p. Mg, C/Mg–1Al, C/AZ31, and C/AZ91 composites, respectively. The fiber strength in C/AZ31 and C/AZ91 composites is significantly decreased in comparison with the raw and/or coated fibers. On the other hand, the fibers in C/c.p. Mg and C/Mg–1Al show less degradation. This variation in tensile strength can be reflected on the change in the microstructures of carbon fibers extracted from the corresponding matrices. It can be observed from the SEM analysis (Fig. 5) that the fibers in C/c.p. Mg and C/Mg–1Al (Fig. 5b–c) are almost intact in comparison with that of raw fibers, except for the appearance of few unknown particles on the fiber surface. These particles are identified and confirmed as residual magnesium matrix by EDS analysis.
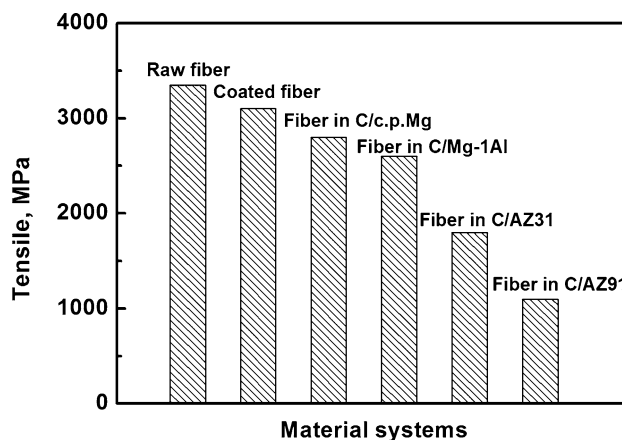

Fig. 4 Comparison of tensile strength between raw fiber, coated fiber, and coated fiber in C/c.p. Mg, C/Mg–1Al, C/AZ31, and C/AZ91 composites, respectively
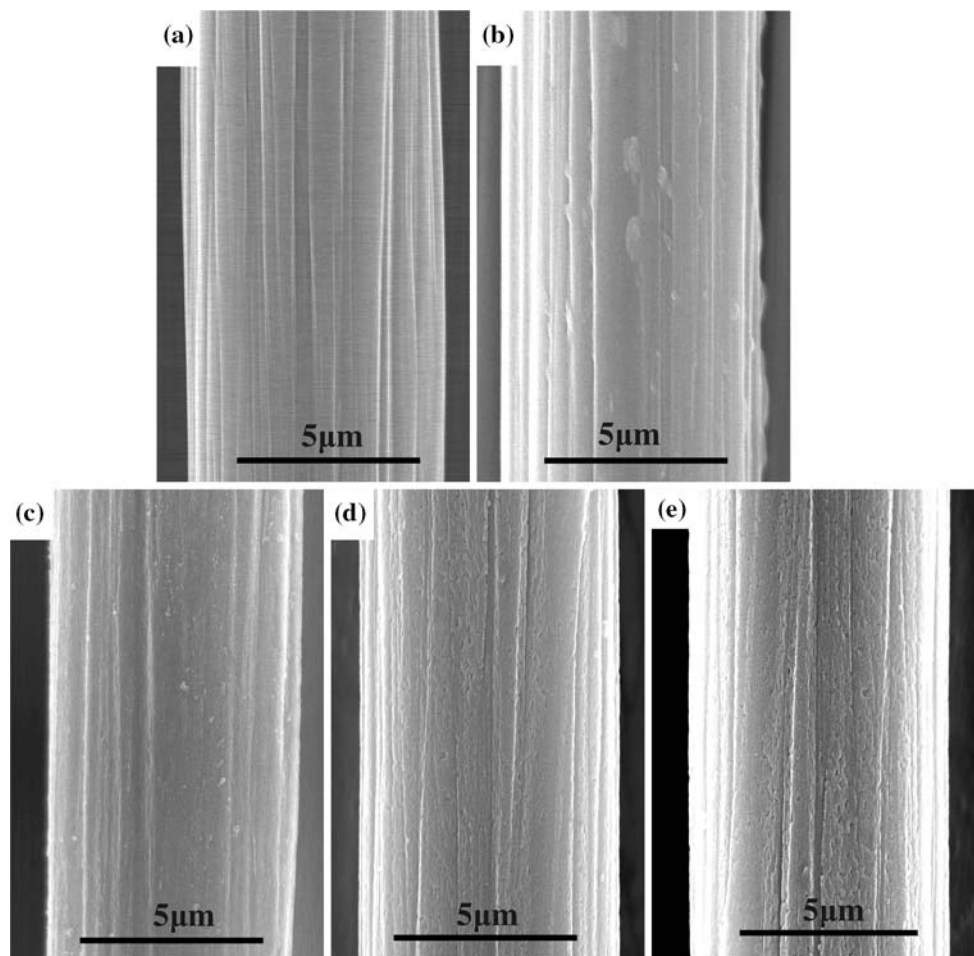
Fig. 5 SEM images of raw fiber (**a**) and carbon fibers extracted from composites: **b** C/c.p. Mg, **c** C/Mg–1Al, **d** C/AZ31, and **e** C/AZ91

In addition, numerous erosion pits were observed over the surface of the carbon fiber in C/AZ31 and C/AZ91 composite (Fig. 5d, e). It is known that the interfacial reaction product, namely aluminum carbide, can be easily dissolved in water during the composite etching. Hence, the obtained notching effect (erosion pits) probably resulted from the removal of the carbides caused by interfacial chemical reaction, which is further supported by the TEM observation described below.

Composite interface and microstructure

Figure 6a demonstrates the interfacial microstructure of C/c.p. Mg obtained from TEM analysis. A distinct interface layer is observed between carbon fiber and matrix. EDS and electron diffraction analysis (Fig. 6b) reveal that the interfacial layer is composed of an amorphous SiO_2 coating and MgO phase. The chemical reaction ($2Mg + SiO_2 \rightarrow 2MgO + Si, G(670\,^{\circ}C) = -128\,kJmol^{-1}$) [12] suggests that the large amount of oxygen probably arises from the SiO_2 coating rather than the processing methodology. The

presence of passivating MgO interlayer is suggested as beneficial to the wetting/bonding at the fiber/matrix interface [8]. This is probably because the SiO_2 coating serves well as a diffusion barrier. Consequently, the absence of interfacial carbide formation could result in a relatively weak interfacial bonding and extensive fiber pullout as previously shown in Fig. 2a, b.

Figure 7a, b shows the interfacial characteristics of C/Mg–1Al and C/AZ31, respectively. The microstructure of C/Mg–1Al is quite similar to that of C/c.p. Mg, where the remaining SiO_2 coating is very thin. It can also be noticed that the interfacial chemical reaction takes place in local area and some fine precipitates (Fig. 7b) fierce the coatings. Therefore, network structure of SiO_2 probably requires denser or more compact coatings in practical applications, especially for C/Mg–Al composites with higher Al content. Moreover, it is difficult to identify the existence of SiO_2 coating in C/AZ31 composite and the needle-shaped precipitates are visible near the interface. Furthermore, it is also observed that the remaining Al would induce the formation of Mg–Al inter-metallic,
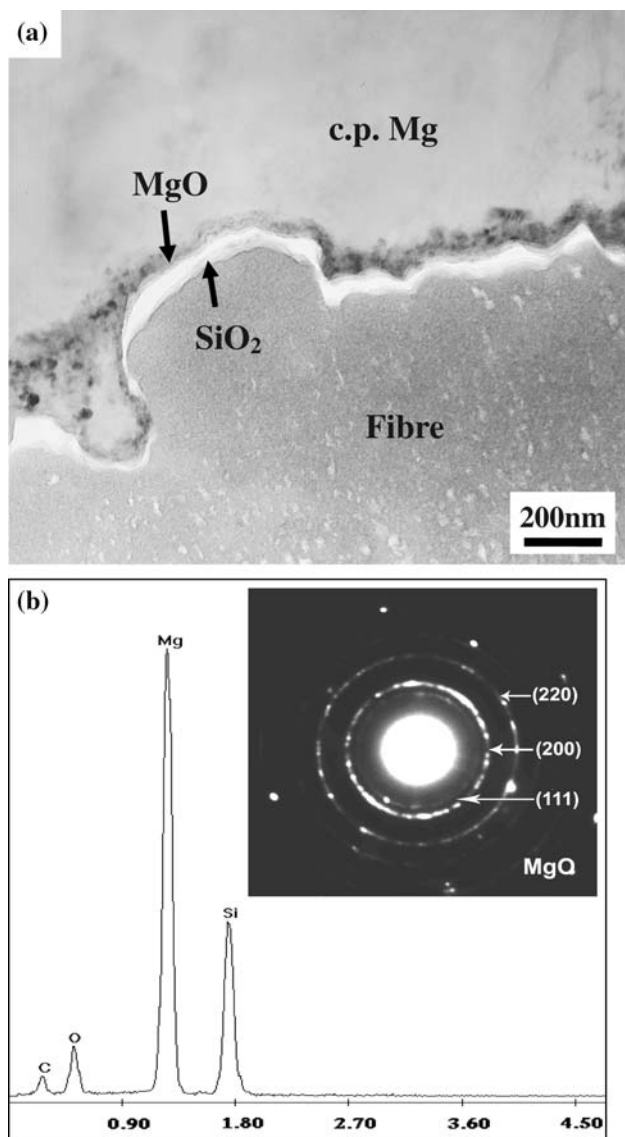
Fig. 6 TEM images corresponding to the interface area: **a** coated C/c.p. Mg composite and **b** selected area diffraction patterns and EDS spectrum

Fig. 7 TEM image showing the interfacial characteristics of **a** C/Mg–1Al and **b** C/AZ31

$Mg_{17}Al_{12}$ (β), in the magnesium matrix as suggested by TEM analysis in Fig. 8. However, the β precipitates are inhomogeneous and nucleate close to the interface [7]. This is contradicted from the study by Wu et al. [8], where the precipitates appear at a remote point from the interface.

The fracture behavior of C/AZ91 can be further explained by the interfacial characteristics (based on higher fiber/matrix reactivity), where many lath-shaped precipitates are visible with a maximum width of 50 nm and an approximate length of 600 nm (see Fig. 9). These precipitates are significantly varied from the aforementioned ones by both quantity and size. In most cases, these precipitates are concentrated on the fiber surfaces and extended into the matrix. At these locations, 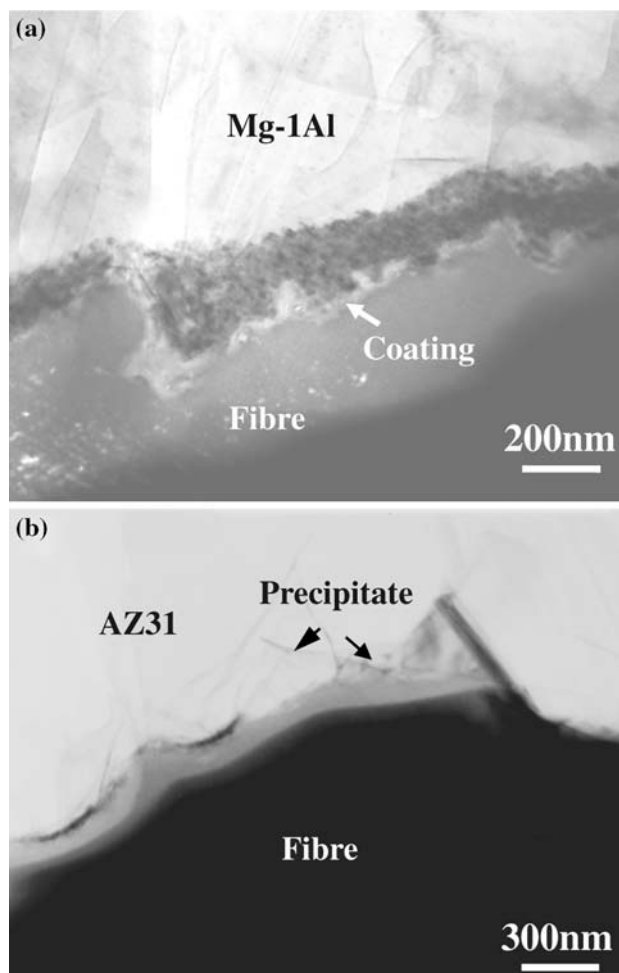notching effect could occur directly on the fiber surface by the carbides that might contribute to the fiber degradation (see Fig. 5b). Obviously, besides a strong interfacial bonding, these precipitates also embrittle the material leading to deteriorate the mechanical properties of the composite. The formation and compositional analysis of these precipitates are studied extensively [2, 7, 8, 12], and therefore it is only briefly summarized here. Viala et al. [1] have systematically investigated the possible chemical reactions occurred between Mg–Al and carbon fibers. They have suggested that aluminum carbide (Al_4C_3) might be formed in the alloys with Al content ranging from 0.6 wt% to 19 wt%. By using electron energy loss (EEL) spectroscopy methods, Feldhoff et al. [4] suggested that the formation of the ternary carbide like Al_2MgC_2 is more favored within this limit. In the present study, the EDS analysis (Fig. 9c) showed that these precipitates mainly consisted of three elements namely carbon, aluminum, and magnesium. The amount of ingredient obtained is analogous to the Al_2MgC_2, and the crystal chemistry is closely related to that of Al_4C_3.
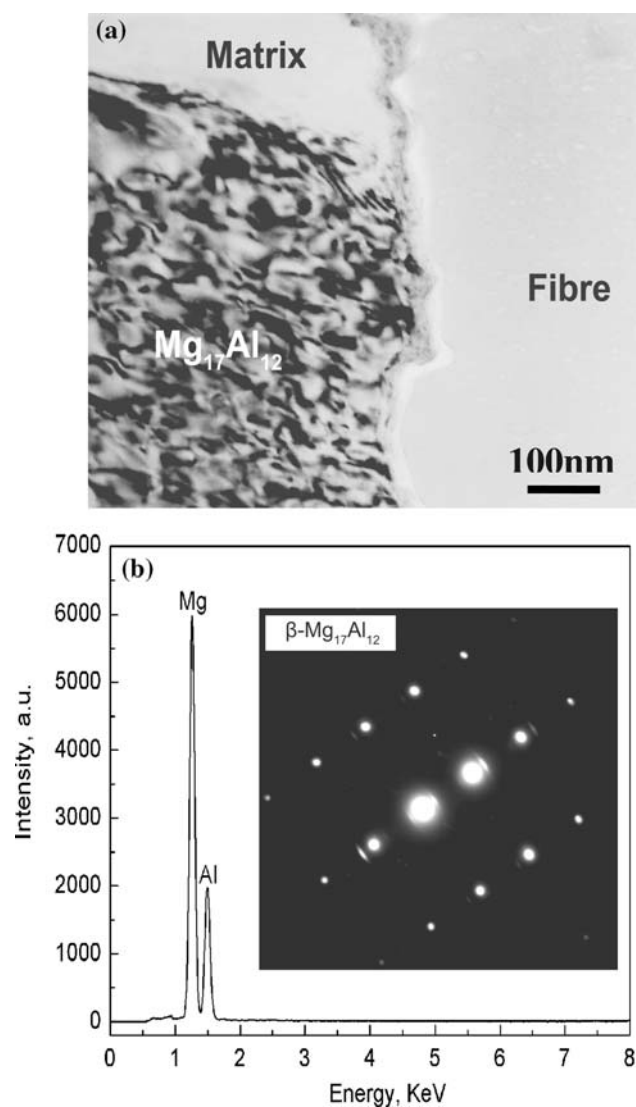
Fig. 8 TEM image showing **a** continuous precipitates near the interface; **b** electron diffraction pattern and EDS spectrum from the same area

The elemental inter-diffusion behavior between matrix and carbon fiber is also analyzed. All the interface regions contain C, O, Mg, and Al elements, and Zn is not detected in the interface probably due to its lower content in the matrix. However, the Al content in the interface region is increased from 5.0 wt% to until 9.6 wt% as its increase in AZ31 and AZ9 matrices, respectively. C is located only in the interface, without further diffusion into the matrix for all the composites. It should be noted that the SiO_2 coating is gradually depleted with the increase of Al content in matrices, as it happened in C/AZ31 and C/AZ91 (see Figs. 6a, 8a, b, and 9a). In this case, it seems that the SiO_2 coating does not function well as diffusion barrier against the magnesium penetration [4]. Although local enrichment of Al around carbon fiber is observed for C/AZ31 and
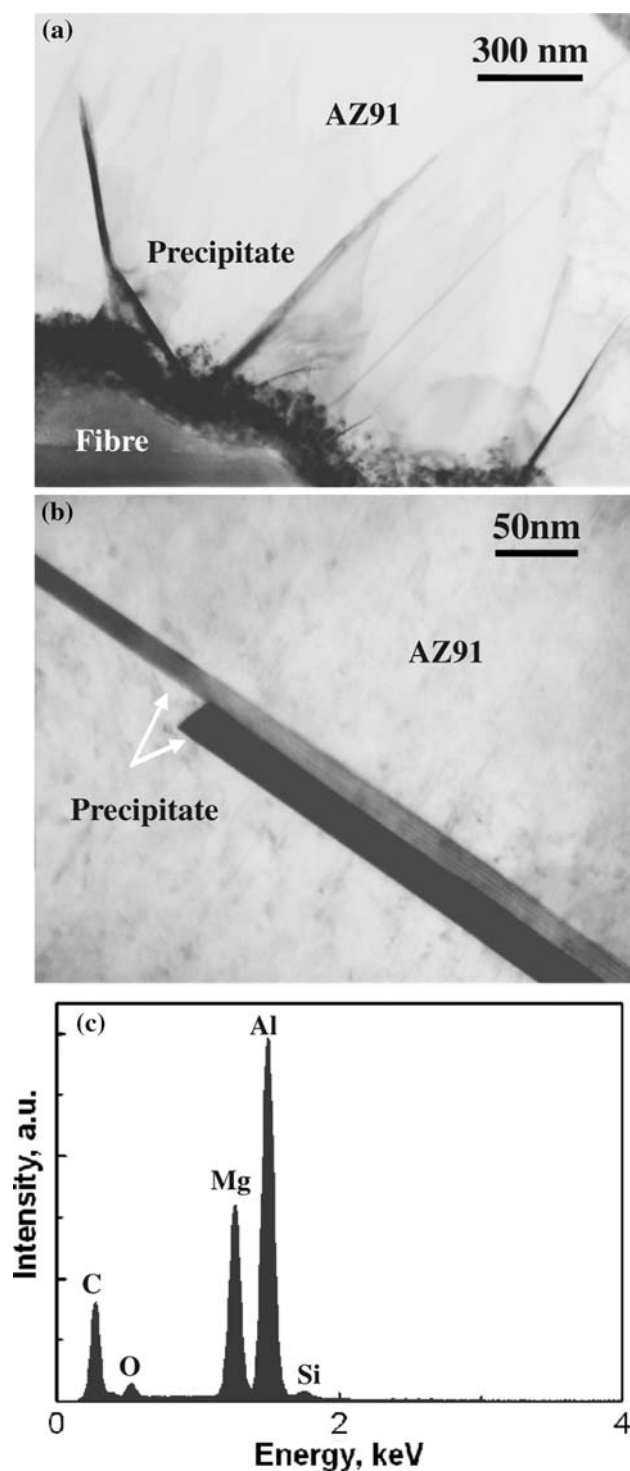

Fig. 9 TEM images showing the interfacial characteristics of **a** C/AZ91, **b** lath-shaped precipitation, and **c** EDS spectrum for precipitation

C/AZ91 as suggested by other reports [2, 4, 7], it is not the same in C/Mg–1Al composite. As it is known, the solubility limit of Al in magnesium matrix is about 12.7 wt% at 437°. The solubility of Al will be significantly decreased as

the temperature drops with the value being ~ 1 wt% at room temperature. Therefore, regarding C/Mg–1Al composite with lower Al level, the Al element was completely dissolved in the matrix with no segregation even after solidification, which explains the preceding phenomenon.

Conclusions

It is demonstrated that in coated carbon fiber-reinforced magnesium composites, the mechanical behavior of the composites can be optimized by varying the aluminum (Al) content in the matrices, so as to yield a moderate chemical activity (minor precipitation) in the interfacial region connected with a bundle pull-out behavior. For C/commercially pure Mg composite, the fracture behavior was characterized by a large amount of fiber pull-out. This is indicating a weak interface bonding, in which the SiO_2 coating serves as a good barrier to elemental diffusion in the system. When the Al content in the matrix is increased to 1 wt%, the alloy element is completely dissolved and the C/Mg–1Al composite provides the best mechanical performance with suitable interface tailoring. On the contrary, in the C/Mg–Al composites with higher Al content such as AZ31 and AZ91, the SiO_2 coatings are fully depleted due to the extensive formation of carbides in the interface and the composites exhibit brittle fracture behavior as well as lower tensile strength. Further, the precipitates are identified as Al_2MgC_2 phase, similar to binary carbide (Al_4C_3).

References

1. Viala JC, Fortier P, Claveyrolas G, Vincent H, Bouix J (1991) J Mater Sci 26:4977. doi:10.1007/BF00549880
2. Feldhoff A, Pippel E, Woltersdorf J (1999) J Micro 196:185
3. Katzman HA (1987) J Mater Sci 22:144. doi:10.1007/BF01160563
4. Feldhoff A, Pippel E, Woltersdorf J (2000) Adv Eng Mater 2:471
5. Chen R, Li XG (1993) Comp Sci Technol 49:357
6. Wu F, Zhu J, Chen Y, Zhang GD (2000) Mater Sci Eng A 277:143
7. Stevens MR, Todd R, Papakyriacou M (2005) Surf Interface Anal 37:336
8. Wu F, Zhu J (1997) Comp Sci Technol 57:661
9. Gao PZ, Wang HJ, Jin ZH (2003) J Inorg Mater 18:849
10. Li HL, Mao ZY, Peng HY, Shang BL (1991) Mater Sci Process 5:271
11. Diwanji AP, Hall IW (1992) J Mater Sci 27:2093. doi:10.1007/BF01117922
12. Kleine A, Hemptenmacher J, Dudek HJ, Kainer KU, Krüger G (1995) J Mater Sci Lett 14:358